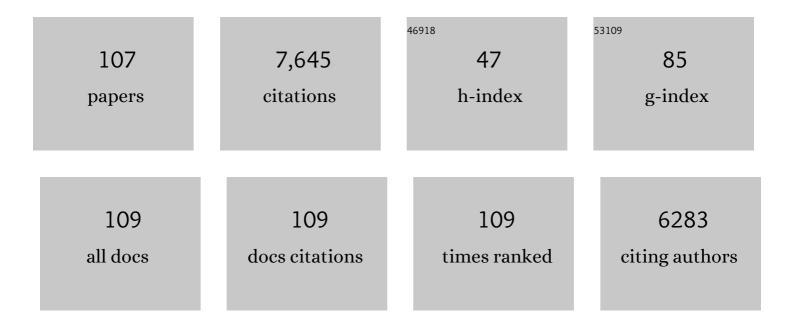
List of Publications by Year in descending order

Source: https://exaly.com/author-pdf/3053114/publications.pdf Version: 2024-02-01



#	Article	IF	CITATIONS
1	Hybrid graphene aerogels/phase change material composites: Thermal conductivity, shape-stabilization and light-to-thermal energy storage. Carbon, 2016, 100, 693-702.	5.4	351
2	Smart Ti ₃ C ₂ T _{<i>x</i>} MXene Fabric with Fast Humidity Response and Joule Heating for Healthcare and Medical Therapy Applications. ACS Nano, 2020, 14, 8793-8805.	7.3	288
3	Stereocomplex Crystallite Network in Asymmetric PLLA/PDLA Blends: Formation, Structure, and Confining Effect on the Crystallization Rate of Homocrystallites. Macromolecules, 2014, 47, 1439-1448.	2.2	267
4	Largely enhanced thermal conductivity of poly (ethylene glycol)/boron nitride composite phase change materials for solar-thermal-electric energy conversion and storage with very low content of graphene nanoplatelets. Chemical Engineering Journal, 2017, 315, 481-490.	6.6	264
5	Hybrid network structure of boron nitride and graphene oxide in shape-stabilized composite phase change materials with enhanced thermal conductivity and light-to-electric energy conversion capability. Solar Energy Materials and Solar Cells, 2018, 174, 56-64.	3.0	223
6	An ice-templated assembly strategy to construct graphene oxide/boron nitride hybrid porous scaffolds in phase change materials with enhanced thermal conductivity and shape stability for light–thermal–electric energy conversion. Journal of Materials Chemistry A, 2016, 4, 18841-18851.	5.2	216
7	Flexible Anti-Biofouling MXene/Cellulose Fibrous Membrane for Sustainable Solar-Driven Water Purification. ACS Applied Materials & Interfaces, 2019, 11, 36589-36597.	4.0	216
8	Hybridizing graphene aerogel into three-dimensional graphene foam for high-performance composite phase change materials. Energy Storage Materials, 2018, 13, 88-95.	9.5	210
9	Macroporous three-dimensional MXene architectures for highly efficient solar steam generation. Journal of Materials Chemistry A, 2019, 7, 10446-10455.	5.2	208
10	Hierarchical graphene foam-based phase change materials with enhanced thermal conductivity and shape stability for efficient solar-to-thermal energy conversion and storage. Nano Research, 2017, 10, 802-813.	5.8	206
11	Self-assembled high-strength hydroxyapatite/graphene oxide/chitosan composite hydrogel for bone tissue engineering. Carbohydrate Polymers, 2017, 155, 507-515.	5.1	205
12	Enhanced comprehensive performance of polyethylene glycol based phase change material with hybrid graphene nanomaterials for thermal energy storage. Carbon, 2015, 88, 196-205.	5.4	189
13	High-performance composite phase change materials for energy conversion based on macroscopically three-dimensional structural materials. Materials Horizons, 2019, 6, 250-273.	6.4	187
14	Multilayer structured AgNW/WPU-MXene fiber strain sensors with ultrahigh sensitivity and a wide operating range for wearable monitoring and healthcare. Journal of Materials Chemistry A, 2019, 7, 15913-15923.	5.2	184
15	Polyethylene glycol based shape-stabilized phase change material for thermal energy storage with ultra-low content of graphene oxide. Solar Energy Materials and Solar Cells, 2014, 123, 171-177.	3.0	178
16	Self-assembled core-shell polydopamine@MXene with synergistic solar absorption capability for highly efficient solar-to-vapor generation. Nano Research, 2020, 13, 255-264.	5.8	174
17	Boosting piezoelectric response of PVDF-TrFE via MXene for self-powered linear pressure sensor. Composites Science and Technology, 2021, 202, 108600.	3.8	165
18	Novel photodriven composite phase change materials with bioinspired modification of BN for solar-thermal energy conversion and storage. Journal of Materials Chemistry A, 2016, 4, 9625-9634.	5.2	163

#	Article	IF	CITATIONS
19	All-weather-available, continuous steam generation based on the synergistic photo-thermal and electro-thermal conversion by MXene-based aerogels. Materials Horizons, 2020, 7, 855-865.	6.4	153
20	Hierarchically interconnected porous scaffolds for phase change materials with improved thermal conductivity and efficient solar-to-electric energy conversion. Nanoscale, 2017, 9, 17704-17709.	2.8	131
21	Multifunctional Thermal Management Materials with Excellent Heat Dissipation and Generation Capability for Future Electronics. ACS Applied Materials & Interfaces, 2019, 11, 18739-18745.	4.0	116
22	Self-Assembled Sponge-like Chitosan/Reduced Graphene Oxide/Montmorillonite Composite Hydrogels without Cross-Linking of Chitosan for Effective Cr(VI) Sorption. ACS Sustainable Chemistry and Engineering, 2017, 5, 1557-1566.	3.2	111
23	A bridge-arched and layer-structured hollow melamine foam/reduced graphene oxide composite with an enlarged evaporation area and superior thermal insulation for high-performance solar steam generation. Journal of Materials Chemistry A, 2020, 8, 2701-2711.	5.2	103
24	Polyethylene glycol/graphene oxide aerogel shape-stabilized phase change materials for photo-to-thermal energy conversion and storage via tuning the oxidation degree of graphene oxide. Energy Conversion and Management, 2017, 146, 253-264.	4.4	99
25	Temperature induced gelation transition of a fumed silica/PEG shear thickening fluid. RSC Advances, 2015, 5, 18367-18374.	1.7	94
26	Polymorphism of Racemic Poly(<scp>l</scp> -lactide)/Poly(<scp>d</scp> -lactide) Blend: Effect of Melt and Cold Crystallization. Journal of Physical Chemistry B, 2013, 117, 3667-3674.	1.2	93
27	A new approach to construct segregated structures in thermoplastic polyolefin elastomers towards improved conductive and mechanical properties. Journal of Materials Chemistry A, 2015, 3, 5482-5490.	5.2	91
28	Recent advances in polymer-based thermal interface materials for thermal management: A mini-review. Composites Communications, 2020, 22, 100528.	3.3	91
29	Photodriven Shape-Stabilized Phase Change Materials with Optimized Thermal Conductivity by Tailoring the Microstructure of Hierarchically Ordered Hybrid Porous Scaffolds. ACS Sustainable Chemistry and Engineering, 2018, 6, 6761-6770.	3.2	88
30	Bacterial cellulose/MXene hybrid aerogels for photodriven shape-stabilized composite phase change materials. Solar Energy Materials and Solar Cells, 2019, 203, 110174.	3.0	85
31	Electrically insulating POE/BN elastomeric composites with high through-plane thermal conductivity fabricated by two-roll milling and hot compression. Advanced Composites and Hybrid Materials, 2018, 1, 160-167.	9.9	81
32	Effect of temperature, crystallinity and molecular chain orientation on the thermal conductivity of polymers: a case study of PLLA. Journal of Materials Science, 2018, 53, 10543-10553.	1.7	79
33	Human Skin-Inspired Electronic Sensor Skin with Electromagnetic Interference Shielding for the Sensation and Protection of Wearable Electronics. ACS Applied Materials & Interfaces, 2018, 10, 40880-40889.	4.0	78
34	A strain localization directed crack control strategy for designing MXene-based customizable sensitivity and sensing range strain sensors for full-range human motion monitoring. Nano Energy, 2020, 74, 104814.	8.2	77
35	Recent Advances in Multiresponsive Flexible Sensors towards Eâ€skin: A Delicate Design for Versatile Sensing. Small, 2022, 18, e2103734.	5.2	76
36	Towards balanced strength and toughness improvement of isotactic polypropylene nanocomposites by surface functionalized graphene oxide. Journal of Materials Chemistry A, 2014, 2, 3190-3199.	5.2	70

#	Article	IF	CITATIONS
37	Enhancing Thermomechanical Properties and Heat Distortion Resistance of Poly(<scp>l</scp> -lactide) with High Crystallinity under High Cooling Rate. ACS Sustainable Chemistry and Engineering, 2015, 3, 654-661.	3.2	67
38	Low percolation threshold and balanced electrical and mechanical performances in polypropylene/carbon black composites with a continuous segregated structure. Composites Part B: Engineering, 2016, 99, 348-357.	5.9	67
39	Tannic acid functionalized graphene hydrogel for organic dye adsorption. Ecotoxicology and Environmental Safety, 2018, 165, 299-306.	2.9	66
40	Electro and Light-Active Actuators Based on Reversible Shape-Memory Polymer Composites with Segregated Conductive Networks. ACS Applied Materials & Interfaces, 2019, 11, 30332-30340.	4.0	66
41	Robust polymer-based paper-like thermal interface materials with a through-plane thermal conductivity over 9ÂWmâ^'1Kâ^'1. Chemical Engineering Journal, 2020, 392, 123784.	6.6	66
42	Nanofibrillar Poly(vinyl alcohol) Ionic Organohydrogels for Smart Contact Lens and Human-Interactive Sensing. ACS Applied Materials & Interfaces, 2020, 12, 23514-23522.	4.0	59
43	A Facile Route to Fabricate Highly Anisotropic Thermally Conductive Elastomeric POE/NG Composites for Thermal Management. Advanced Materials Interfaces, 2018, 5, 1700946.	1.9	56
44	The enhanced nucleating ability of carbon nanotube-supported β-nucleating agent in isotactic polypropylene. Colloid and Polymer Science, 2010, 288, 681-688.	1.0	54
45	Deformation-induced morphology evolution during uniaxial stretching of isotactic polypropylene: effect of temperature. Colloid and Polymer Science, 2012, 290, 261-274.	1.0	50
46	Tuning the structure of graphene oxide and the properties of poly(vinyl alcohol)/graphene oxide nanocomposites by ultrasonication. Journal of Materials Chemistry A, 2013, 1, 3163.	5.2	49
47	Hierarchically Porous PVA Aerogel for Leakage-Proof Phase Change Materials with Superior Energy Storage Capacity. Energy & Fuels, 2020, 34, 2471-2479.	2.5	49
48	Surface structure engineering for a bionic fiber-based sensor toward linear, tunable, and multifunctional sensing. Materials Horizons, 2020, 7, 2450-2459.	6.4	47
49	High-performance porous polylactide stereocomplex crystallite scaffolds prepared by solution blending and salt leaching. Materials Science and Engineering C, 2018, 90, 602-609.	3.8	46
50	Dopamine-induced functionalization of cellulose nanocrystals with polyethylene glycol towards poly(L-lactic acid) bionanocomposites for green packaging. Carbohydrate Polymers, 2019, 203, 275-284.	5.1	45
51	Achieving improved electromagnetic interference shielding performance and balanced mechanical properties in polyketone nanocomposites via a composite MWCNTs carrier. Composites Part A: Applied Science and Manufacturing, 2020, 136, 105967.	3.8	43
52	Electrical properties and morphology of carbon black filled PP/EPDM blends: effect of selective distribution of fillers induced by dynamic vulcanization. Journal of Materials Science, 2013, 48, 4942-4951.	1.7	42
53	A high-performance temperature sensitive TPV/CB elastomeric composite with balanced electrical and mechanical properties via PF-induced dynamic vulcanization. Journal of Materials Chemistry A, 2014, 2, 16989-16996.	5.2	42
54	Low-entropy structured wearable film sensor with piezoresistive-piezoelectric hybrid effect for 3D mechanical signal screening. Nano Energy, 2021, 90, 106603.	8.2	41

#	Article	IF	CITATIONS
55	Effects of annealing on structure and deformation mechanism of isotactic polypropylene film with rowâ€nucleated lamellar structure. Journal of Applied Polymer Science, 2013, 130, 1659-1666.	1.3	40
56	Greatly accelerated crystallization of poly(lactic acid): cooperative effect of stereocomplex crystallites and polyethylene glycol. Colloid and Polymer Science, 2014, 292, 163-172.	1.0	40
57	High-melting-point crystals of poly(<scp>l</scp> -lactic acid) (PLLA): the most efficient nucleating agent to enhance the crystallization of PLLA. CrystEngComm, 2015, 17, 2310-2320.	1.3	39
58	Phase change mediated mechanically transformative dynamic gel for intelligent control of versatile devices. Materials Horizons, 2021, 8, 1230-1241.	6.4	39
59	An extremely uniform dispersion of MWCNTs in olefin block copolymers significantly enhances electrical and mechanical performances. Polymer Chemistry, 2015, 6, 7160-7170.	1.9	38
60	Poly(l-lactic acid)-polyethylene glycol-poly(l-lactic acid) triblock copolymer: A novel macromolecular plasticizer to enhance the crystallization of poly(l-lactic acid). European Polymer Journal, 2017, 97, 272-281.	2.6	37
61	Templateâ€Free Selfâ€Caging Nanochemistry for Largeâ€6cale Synthesis of Sulfonatedâ€Graphene@Sulfur Nanocage for Longâ€Life Lithiumâ€6ulfur Batteries. Advanced Functional Materials, 2021, 31, 2008652.	7.8	37
62	Tailoring Crystalline Morphology by High-Efficiency Nucleating Fiber: Toward High-Performance Poly(<scp>l</scp> -lactide) Biocomposites. ACS Applied Materials & Interfaces, 2018, 10, 20044-20054.	4.0	36
63	Scalable Flexible Phase Change Materials with a Swollen Polymer Network Structure for Thermal Energy Storage. ACS Applied Materials & Interfaces, 2021, 13, 59364-59372.	4.0	36
64	Flexible phase change hydrogels for mid-/low-temperature infrared stealth. Chemical Engineering Journal, 2022, 446, 137463.	6.6	34
65	Enhanced Thermal Conductivity and Balanced Mechanical Performance of PP/BN Composites with 1 vol% Finely Dispersed MWCNTs Assisted by OBC. Advanced Materials Interfaces, 2019, 6, 1900081.	1.9	33
66	Scalable fabrication of flexible piezoresistive pressure sensors based on occluded microstructures for subtle pressure and force waveform detection. Journal of Materials Chemistry C, 2020, 8, 16774-16783.	2.7	32
67	Polymorphism of a high-molecular-weight racemic poly(<scp>l</scp> -lactide)/poly(<scp>d</scp> -lactide) blend: effect of melt blending with poly(methyl) Tj ETQq1	1 Q.7 7843	14agBT /Ove
68	Suppressing phase coarsening in immiscible polymer blends using nano-silica particles located at the interface. RSC Advances, 2015, 5, 74295-74303.	1.7	30
69	A Green and Facile Melt Approach for Hierarchically Porous Polylactide Monoliths Based on Stereocomplex Crystallite Network. ACS Sustainable Chemistry and Engineering, 2017, 5, 8334-8343.	3.2	30
70	Induced formation of polar phases in poly(vinylidene fluoride) by cetyl trimethyl ammonium bromide. Journal of Materials Science, 2014, 49, 4171-4179.	1.7	29
71	Progress in polyketone materials: blends and composites. Polymer International, 2018, 67, 1478-1487.	1.6	26
72	Highly thermally conductive electrospun stereocomplex polylactide fibrous film dip-coated with silver nanowires. Polymer, 2020, 194, 122390.	1.8	25

#	Article	IF	CITATIONS
73	Supercooling-dependent morphology evolution of an organic nucleating agent in poly(<scp>l</scp> -lactide)/poly(<scp>d</scp> -lactide) blends. CrystEngComm, 2017, 19, 1648-1657.	1.3	24
74	Effect of cross-linking degree of EPDM phase on the electrical properties and formation of dual networks of thermoplastic vulcanizate composites based on isotactic polypropylene (iPP)/ethylene–propylene–diene rubber (EPDM) blends. RSC Advances, 2016, 6, 74567-74574.	1.7	23
75	Balanced strength and ductility improvement of in situ crosslinked polylactide/poly(ethylene) Tj ETQq1 1 0.78	4314 rgBT / 1.7	Overlock 10
76	Synergistic effect of stereocomplex crystals and shear flow on the crystallization rate of poly(I-lactic acid): A rheological study. RSC Advances, 2014, 4, 2733-2742.	1.7	20
77	Suppressing phase retraction and coalescence of co-continuous polymer blends: effect of nanoparticles and particle network. RSC Advances, 2014, 4, 49429-49441.	1.7	20
78	Effect of graphite oxide structure on the formation of stable self-assembled conductive reduced graphite oxide hydrogel. Journal of Materials Chemistry C, 2014, 2, 3846.	2.7	20
79	Direct modification of polyketone resin for anion exchange membrane of alkaline fuel cells. Journal of Colloid and Interface Science, 2019, 556, 420-431.	5.0	20
80	The preparation, structures, and properties of poly(vinylidene fluoride)/multiwall carbon nanotubes nanocomposites. Journal of Applied Polymer Science, 2012, 125, E592.	1.3	19
81	Enantiomeric poly(<scp>d</scp> -lactide) with a higher melting point served as a significant nucleating agent for poly(<scp>l</scp> -lactide). CrystEngComm, 2015, 17, 4334-4342.	1.3	19
82	Effect of chain entanglement on the melt-crystallization behavior of poly(l-lactide) acid. Journal of Polymer Research, 2016, 23, 1.	1.2	19
83	Effect of aspect ratio of multi-wall carbon nanotubes on the dispersion in ethylene-α-octene block copolymer and the properties of the Nanocomposites. Journal of Polymer Research, 2019, 26, 1.	1.2	19
84	Leakage-Proof and Malleable Polyethylene Wax Vitrimer Phase Change Materials for Thermal Interface Management. ACS Applied Energy Materials, 2021, 4, 11173-11182.	2.5	19
85	Self-Sensing Actuators Based on a Stiffness Variable Reversible Shape Memory Polymer Enabled by a Phase Change Material. ACS Applied Materials & Interfaces, 2022, 14, 22521-22530.	4.0	19
86	Electrospun Modified Polyketone-Based Anion Exchange Membranes with High Ionic Conductivity and Robust Mechanical Properties. ACS Applied Energy Materials, 2021, 4, 5187-5200.	2.5	18
87	Vitrimers of polyolefin elastomer with physically cross-linked network. Journal of Polymer Research, 2021, 28, 1.	1.2	17
88	Effect of repetitive processing on the mechanical properties and fracture toughness of dynamically vulcanized iPP/EPDM blends. Journal of Applied Polymer Science, 2011, 120, 86-94.	1.3	16
89	Nanoparticle retarded shape relaxation of dispersed droplets in polymer blends: an understanding from the viewpoint of molecular movement. RSC Advances, 2014, 4, 41059-41068.	1.7	15
90	Temperature: a nonnegligible factor for the formation of a structurally stable, self-assembled reduced graphite oxide hydrogel. RSC Advances, 2015, 5, 10-15.	1.7	13

#	Article	IF	CITATIONS
91	Boosting solar steam generation in dynamically tunable polymer porous architectures. Polymer, 2021, 226, 123811.	1.8	13
92	Nitrogen-doped carbon-coated Fe3O4/rGO nanocomposite anode material for enhanced initial coulombic efficiency of lithium-ion batteries. Ionics, 2019, 25, 1513-1521.	1.2	11
93	Constructing Sandwich-Architectured Poly(<scp> </scp> -lactide)/High-Melting-Point Poly(<scp> </scp> -lactide) Nonwoven Fabrics: Toward Heat-Resistant Poly(<scp> </scp> -lactide) Barrier Biocomposites with Full Biodegradability. ACS Applied Bio Materials, 2019, 2, 1357-1367.	2.3	11
94	Biobinder Nanocoating for Upgrading the Assembling Structures of High-Capacity Composite Electrodes with a Robust Polymeric Artificial Solid Electrolyte Interphase. ACS Applied Materials & Interfaces, 2020, 12, 58201-58211.	4.0	11
95	Imidazole-functionalized polyketone-based polyelectrolytes with efficient ionic channels and superwettability for alkaline polyelectrolyte fuel cells and multiple liquid purification. Journal of Materials Chemistry A, 2021, 9, 14827-14840.	5.2	11
96	Insight into the nucleating and reinforcing efficiencies of carbon nanofillers in poly(vinylidene) Tj ETQq0 0 0 rgBT 2013, 48, 8509-8519.	/Overlock 1.7	10 Tf 50 54 10
97	Photo-Driven Self-Healing of Arbitrary Nondestructive Damage in Polyethylene-Based Nanocomposites. ACS Applied Materials & Interfaces, 2020, 12, 1650-1657.	4.0	9
98	Crystallization kinetics of γ phase poly(vinylidene fluoride)(PVDF) induecd by tetrabutylammonium bisulfate. Journal of Polymer Research, 2014, 21, 1.	1.2	8
99	Scalable Synthesis of an Artificial Polydopamine Solidâ€Electrolyteâ€Interfaceâ€Assisted 3D rGO/Fe ₃ O ₄ @PDA Hydrogel for a Highly Stable Anode with Enhanced Lithiumâ€Ionâ€Storage Properties. ChemElectroChem, 2019, 6, 1069-1077.	1.7	8
100	Degradable ultrathin high-performance photocatalytic hydrogen generator from porous electrospun composite fiber membrane with enhanced light absorption ability. Journal of Materials Chemistry A, 2021, 9, 10277-10288.	5.2	8
101	Tunable reversible deformation of semicrystalline polymer networks based on temperature memory effect. Polymer, 2021, 232, 124157.	1.8	7
102	Studies on the Blends of Polyamide66 and Thermoplastic Polyimide. Journal of Macromolecular Science - Physics, 2010, 49, 629-639.	0.4	5
103	Morphologies, interfacial interaction and mechanical performance of super-tough nanostructured PK/PA6 blends. Polymer Testing, 2020, 91, 106777.	2.3	5
104	In situ interfacial engineering enabled mechanically adaptive and highly stretchable liquid metal conductor. Polymer, 2022, 240, 124482.	1.8	3
105	Hierarchical Distribution of β-Phase in Compression- and Injection-Molded, Polypropylene-Based TPV. Journal of Macromolecular Science - Physics, 2010, 50, 62-74.	0.4	2
106	Solvent-controlled formation of a reduced graphite oxide gel via hydrogen bonding. RSC Advances, 2016, 6, 27267-27271.	1.7	2
107	Excellent mechanical performance and enhanced dielectric properties of OBC/SiO2 elastomeric nanocomposites: effect of dispersion of the SiO2 nanoparticles. RSC Advances, 2017, 7, 46297-46305.	1.7	2